J|A|C|S ARTICLES

Published on Web 06/10/2010

# Hindered Rotation of a Cofactor Methyl Group as a Probe for Protein−Cofactor Interaction

Richard Brosi,[†] Boris Illarionov,[‡] Tilo Mathes,[§] Markus Fischer,[‡] Monika Joshi,[||] Adelbert Bacher,[||] Peter Hegemann,[§] Robert Bittl,[†] Stefan Weber,[⊥] and Erik Schleicher*[,⊥]

*Fachbereich Physik, Institut für Experimentalphysik, Freie Universität Berlin, Arnimallee 14, 14195 Berlin, Germany, Institut für Lebensmittelchemie, Universität Hamburg, Grindelallee 117, 20146 Hamburg, Germany, Fachbereich Biologie, Institut für experimentelle Biophysik, Humboldt-Universität zu Berlin, Invalidenstrasse 42, 10115 Berlin, Germany, Department Chemie, Technische Universität München, Lichtenbergstrasse 4, 85747 Garching, Germany, and Institut für Physikalische Chemie, Albert-Ludwigs-Universität Freiburg, Albertstrasse 21, 79104 Freiburg, Germany*

Received December 27, 2009; E-mail: erik.schleicher@physchem.uni-freiburg.de

***Abstract:*** Exploring protein−cofactor interactions on a molecular level is one of the major challenges in modern biophysics. Based on structural data alone it is rarely possible to identify how subtle interactions between a protein and its cofactor modulate the protein's reactivity. In the case of enzymatic processes in which paramagnetic molecules play a certain role, EPR and related methods such as ENDOR are suitable techniques to unravel such important details. In this contribution, we describe how cryogenic-temperature ENDOR spectroscopy can be applied to various LOV domains, the blue-light sensing domains of phototropin photoreceptors, to gain information on the direct vicinity of the flavin mononucleotide (FMN) cofactor by analyzing the temperature dependence of methyl-group rotation attached to C(8) of the FMN's isoalloxazine ring. More specifically, mutational studies of three amino acids surrounding the methyl group led to the identification of Asn425 as an important amino acid that critically influences the dark-state recovery of *Avena sativa* LOV2 domains. Consequently, it is possible to probe protein−cofactor interactions on a sub-angstrom level by following the temperature dependencies of hyperfine couplings.

## Introduction

Phototropins[1] are one of the three known families of flavoproteins mediating blue-light perception:[2] (i) "blue-light using FAD" (BLUF) domains, which are mainly found in bacteria and algae;[3] (ii) cryptochromes expressed in bacteria, plants, and mammals;[4] and (iii) phototropins, which are most prevalent in prokaryotes and plants.[5] Proteins from the plant phototropin superfamily consist of three conserved domains: two so-called "light, oxygen, or voltage" (LOV) domains and a C-terminal kinase domain.[6] In prokaryotic systems, LOV-containing photoreceptors have only one LOV domain and one reporter domain,[7] which has most likely kinase activity.[5] More specifically, LOV domains are members of the PAS superfamily,[8] are in the size range of ∼100 amino acids, and noncovalently bind one flavin mononucleotide (FMN) as a light-sensitive cofactor. Phototropins are able to sense an external physical stimulus (light) via their LOV domains and convert it into a biological signal to propagate to downstream components of the cellular signal transduction system via their reporter domain. Blue-light perception in plants is responsible for numerous phenomena including phototropism, chloroplast movement, leaf expansion, rapid growth inhibition, and stomatal opening.[9] In bacteria, blue-light perception results in a multitude of responses, such as regulation of virulence in *Brucella abortus*[10] or general stress response.[11]

The primary photochemical reaction after blue-light illumination of LOV domains involves the formation of a C4a adduct between the FMN cofactor and a neighboring, strictly conserved cysteine residue.[12,13] In detail, fully oxidized FMN absorbs a

[†] Freie Universität Berlin.
[‡] Universität Hamburg.
[§] Humboldt-Universität zu Berlin.
[||] Technische Universität München.
[⊥] Albert-Ludwigs-Universität Freiburg.

(1) Briggs, W. R.; Huala, E. *Annu. Rev. Cell Dev. Biol.* **1999**, *15*, 33–62.
(2) van der Horst, M. A.; Hellingwerf, K. J. *Acc. Chem. Res.* **2004**, *37*, 13–20.
(3) Gomelsky, M.; Klug, G. *Trends Biochem. Sci.* **2002**, *27*, 497–500.
(4) Lin, C.; Todo, T. *Genome Biol.* **2005**, *6*, Art. No. 220.
(5) Briggs, W. R. *J. Biomed. Sci.* **2007**, *14*, 499–504.
(6) Huala, E.; Oeller, P. W.; Liscum, E.; Han, I.-S.; Larsen, E.; Briggs, W. R. *Science* **1997**, *278*, 2120–2123.
(7) Losi, A.; Polverini, E.; Quest, B.; Gärtner, W. *Biophys. J.* **2002**, *82*, 2627–2634.
(8) Gu, Y.-Z.; Hogenesch, J. B.; Bradfield, C. A. *Annu. Rev. Pharmacol. Toxicol.* **2000**, *40*, 519–561.
(9) Briggs, W. R.; Christie, J. M. *Trends Plant Sci.* **2002**, *7*, 204–210.
(10) Swartz, T. E.; Tseng, T.-S.; Frederickson, M. A.; Paris, G.; Comerci, D. J.; Rajashekara, G.; Kim, J.-G.; Mudgett, M. B.; Splitter, G. A.; Ugalde, R. A.; Goldbaum, F. A.; Briggs, W. R.; Bogomolni, R. A. *Science* **2007**, *317*, 1090–1093.
(11) Suzuki, N.; Takaya, N.; Hoshino, T.; Nakamura, A. *J. Gen. Appl. Microbiol.* **2007**, *53*, 81–88.
(12) Salomon, M.; Christie, J. M.; Knieb, E.; Lempert, U.; Briggs, W. R. *Biochemistry* **2000**, *39*, 9401–9410.
(13) Crosson, S.; Moffat, K. *Plant Cell* **2002**, *14*, 1067–1075.

  

photon, leading to an excited singlet state, followed by subsequent intersystem crossing to a triplet excited state.[14] Although there is an ongoing discussion regarding the molecular mechanism of bond formation, electron transfer from the cysteine to the flavin resulting in a transiently formed radical pair followed by proton transfer and subsequent bond formation seems most likely.[15,16]

Still, several major questions regarding phototropin biochemistry remain unanswered. The interaction between LOV1 and LOV2 domains and how the two domains modulate the light-sensing signal are still unknown.[17,18] Moreover, the slow dark-state recovery and the remarkable reaction rate divergence depending on the organism are still incompletely understood.[19] One approach for understanding such phenomena is to assume that minor changes in the protein environment can lead to subtle changes in the energetic stability of protein conformations. These conformational changes in turn could alter the stability of the carbon−sulfur bond and, thus, modulate the reaction speed of the $\Delta G$-driven C−S bond splitting. A number of examples in the literature show significant modulation of adduct formation/bond breaking via point mutations at various sites of the phototropin protein.[20,21] These findings support the idea that subtle structural changes in these receptor domains can cause significant changes in their reactivity.

Although considerable effort was invested to describe the signal transduction from the LOV receptor to the kinase domain, interactions modulating kinase activity have only been partially deciphered before now.[18,22,23] Small light-activated changes in the protein conformation are suspected to initiate signal transduction. For a profound understanding of this unique photochemical reaction, information on the hydrogen-bonding situation and the close environment of the photolabile center is crucial.

The main focus of this contribution is to resolve regions of the microenvironment in the close vicinity of the flavin cofactor and to elucidate their influence on the protein's reactivity. Resolving the microenvironment of cofactors in proteins and its influence on biological function is difficult, as most of these structural changes are on a length scale that is well below the resolution capacity of X-ray crystallography: For instance, the recently published structures of the LOV domain from the fern *Adiantum capillus-veneris* phototropin photoreceptor obtained from dark- and light-adapted crystals exhibit only minute conformational changes,[13] even though molecular spectroscopy is able to detect clear differences between dark and light states of the cofactor.[24−26]

Spectroscopic methods such as NMR generally offer the necessary spectral resolution; we use electron−nuclear double-resonance (ENDOR) spectroscopy, a method combining NMR with electron paramagnetic resonance (EPR), thus enhancing sensitivity and selectivity for paramagnetic states. By detecting hyperfine couplings (hfc's) of the unpaired electron spin with nearby nuclear spins, only paramagnetic molecules and their close surroundings contribute to the spectrum. This can be used as an endogenous probe of any of the nuclei harboring the unpaired electron spin, and thus, information on the hydrogen-bonding situation and on small structural rearrangements during photoreactions can be derived. Specifically, we use a unique spectral behavior of LOV domain samples to gain detailed information on the interaction between the FMN's xylene ring in the isoalloxazine moiety and its surrounding amino acids. To increase structural information extractable from experimental data, we also take its temperature dependence into account. From these data, the internal energy of the system and, hence, the strength of interaction between the cofactor and its surrounding can be estimated. Such knowledge is crucial for understanding the chemical properties of flavins as cofactors in general and the degree of stability of the blue-light-initiated phototropin signal reaction in particular. For this purpose, we use site-directed mutagenesis of LOV domains where the reactive cysteine residue is exchanged with either alanine or serine. This prevents the formation of the C4a adduct and instead leads to a metastable neutral flavin radical (FMNH$^\bullet$), which is proposed to serve as a reaction intermediate analogue.

## Results

**Proton ENDOR Spectroscopy of LOV Domains.** To enable photogenerated formation of a stable flavin radical, the cysteine residues involved in 4a-cysteine adduct formation in the biological photocycle of LOV domains were replaced by serine or alanine in the LOV2 domains of phototropins from *Chlamydomonas reinhardtii* (*Cr*LOV2) and *Avena sativa* LOV2 (*As*LOV2), respectively. The proteins were converted into their blue neutral radical form by blue-light illumination as described in the Experimental Section, and Davies-type proton ENDOR spectra were recorded at X-band frequencies (at magnetic-field values corresponding to the center-magnetic-field position of the pulsed EPR signal shown in Figure S1 in the Supporting Information) at temperatures from 5 to 140 K (see Figure 1). Resonance intensities were normalized for the "matrix" region between about 14 and 16 MHz. Within this 2-MHz range around the proton Larmor frequency of 14.74 MHz, the resonances of all weakly coupled protons (i.e., H3, H7α, and water protons in the close cofactor surroundings) are found.

The spectra of the C250S mutant of *Cr*LOV2 appear essentially invariant over the temperature range from 120 to 40 K (Figure 1a). At lower temperatures, the intensities of the prominent band pattern located around 11 and 18 MHz become,

(14) Swartz, T. E.; Corchnoy, S. B.; Christie, J. M.; Lewis, J. W.; Szundi, I.; Briggs, W. R.; Bogomolni, R. A. *J. Biol. Chem.* **2001**, *276*, 36493–36500.
(15) Schleicher, E.; Kowalczyk, R. M.; Kay, C. W. M.; Hegemann, P.; Bacher, A.; Fischer, M.; Bittl, R.; Richter, G.; Weber, S. *J. Am. Chem. Soc.* **2004**, *126*, 11067–11076.
(16) Kay, C. W. M.; Schleicher, E.; Kuppig, A.; Hofner, H.; Rüdiger, W.; Schleicher, M.; Fischer, M.; Bacher, A.; Weber, S.; Richter, G. *J. Biol. Chem.* **2003**, *278*, 10973–10982.
(17) Matsuoka, D.; Tokutomi, S. *Proc. Natl. Acad. Sci. U.S.A.* **2005**, *102*, 13337–13342.
(18) Tokutomi, S.; Matsuoka, D.; Zikihara, K. *Biochim. Biophys. Acta* **2008**, *1784*, 133–142.
(19) Kasahara, M.; Swartz, T. E.; Olney, M. A.; Onodera, A.; Mochizuki, N.; Fukuzawa, H.; Asamizu, E.; Tabata, S.; Kanegae, H.; Takano, M.; Christie, J. M.; Nagatani, A.; Briggs, W. R. *Plant Physiol.* **2002**, *129*, 762–773.
(20) Jones, M. A.; Feeney, K. A.; Kelly, S. M.; Christie, J. M. *J. Biol. Chem.* **2007**, *282*, 6405–6414.
(21) Christie, J. M.; Corchnoy, S. B.; Swartz, T. E.; Hokenson, M.; Han, I.-S.; Briggs, W. R.; Bogomolni, R. A. *Biochemistry* **2007**, *46*, 9310–9319.
(22) Christie, J. M. *Annu. Rev. Plant Biol.* **2007**, *58*, 21–45.
(23) Yamamoto, A.; Iwata, T.; Sato, Y.; Matsuoka, D.; Tokutomi, S.; Kandori, H. *Biophys. J.* **2009**, *96*, 2771–2778.
(24) Salomon, M.; Eisenreich, W.; Dürr, H.; Schleicher, E.; Knieb, E.; Massey, V.; Rüdiger, W.; Müller, F.; Bacher, A.; Richter, G. *Proc. Natl. Acad. Sci. U.S.A.* **2001**, *98*, 12357–12361.
(25) Harper, S. M.; Neil, L. C.; Day, I. J.; Hore, P. J.; Gardner, K. H. *J. Am. Chem. Soc.* **2004**, *126*, 3390–3391.
(26) Iwata, T.; Nozaki, D.; Tokutomi, S.; Kagawa, T.; Wada, M.; Kandori, H. *Biochemistry* **2003**, *42*, 8183–8191.

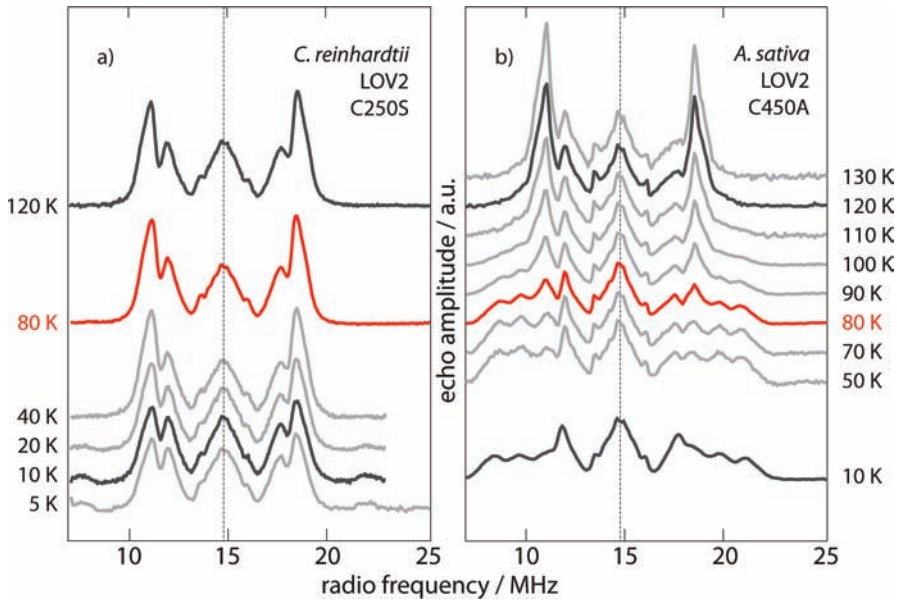


***Figure 1.*** Temperature series of pulsed X-band proton ENDOR spectra obtained from different LOV samples. In each panel, the spectra at 120, 80, and 10 K are highlighted in order to emphasize the very different temperature behavior of (a) the *Cr*LOV2 C250S neutral radical and (b) the *As*LOV2 C450A neutral radical.

in comparison with the intensity of the matrix region around the free proton frequency, progressively smaller; minute additional side bands, which increase with decreasing temperature, appear around 8 and 22 MHz at temperatures below 40 K. By comparison, the spectral changes due to temperature variation are much more dramatic in the case of the C450A mutant protein of *As*LOV2, where the intensity ratio of matrix and side regions already begins to decrease downward from 120 K. Moreover, a complex pattern of new resonances appears below 110 K. To analyze the markedly different temperature sensitivities of the ENDOR spectra of the orthologous proteins under examination, it is required to assign the different spectral components to the respective protons of the flavin chromophore (see Figure 1).

The two prominent features of axial shape in the 10.5−12 and 17.5−19 MHz radio frequency ranges have been attributed to hfc's of the $\beta$-protons (protons in $\beta$-position with respect to the $\pi$-system of the FMN chromophore) of the methyl group attached to C8 of FMN.[16] Typically, methyl groups rotate freely around their C−C bond at elevated temperatures. If this rotation is fast on the ENDOR time scale, one averaged hyperfine (hf) tensor for all three protons of the methyl group is detected in frozen solution. It is therefore tempting to explain the marked temperature dependence of the methyl-group resonances with a formal "slowing-down" of the methyl-group rotation and, at very low temperature, with a complete arrest of the methyl-group motion (on the ENDOR time scale) at specific orientations. However, until now, such phenomena in integral protein−cofactor environments have been expected to occur at liquid helium temperature only. To test the hypothesis that hindered rotation of the 8α-methyl-group protons is responsible for this spectral behavior—unexpected at rather high temperatures—we replaced the FMN chromophore of *As*LOV2 by 8-demethyl-FMN. This implicates the replacement of the three methyl-group $\beta$-protons with a single α-proton (protons in α-position with respect to the $\pi$-system of the FMN chromophore).

8-Demethyl-FMN was synthesized and loaded into *As*LOV2 C450A apoprotein via published procedures,[24,27] which led to a folded yellow protein. UV−vis spectroscopy shows a spectrum similar to spectra obtained from other LOV2 domains,[12,16,19] although the absorption band at 450 nm, which is characteristic for the $S_0$-to-$S_1$ transition of oxidized flavins, is slightly blue-shifted. Moreover, the band around 360 nm arising from the $S_0$-to-$S_2$ transition is blue-shifted by about 15 nm (data not shown). Blue-light illumination of an *As*LOV2 domain loaded with 8-demethyl-FMN results in the formation of a blue neutral semiquinone radical, which was investigated with pulsed ENDOR spectroscopy. As shown in Figure 2a, lower panel, its proton ENDOR spectrum is virtually independent of the temperature over a wide range from 120 to 10 K. This confirms that the temperature-dependent features of protein samples carrying the native FMN cofactor may predominantly and specifically reflect contributions by the protons of the 8α-methyl group. The decrease of intensity at 18 MHz and the correlated appearance of spectral features in the range between 19 and 22 MHz, as observed upon cooling FMN-endowed LOV domains, thus exclusively reflects changes in the hfc's of the three 8α-methyl-group protons.

**Spectral Simulations of ENDOR Spectra from AsLOV2 Mutants.** To address the temperature-dependent changes in the ENDOR spectra in more detail, we used numerical simulations of the *As*LOV2 data from samples complexed to FMN or 8-demethyl-FMN, using a laboratory-written ENDOR simulation program based on the "EasySpin" program package.[28] As the spectral region between 19 and 22 MHz harbors not only the proton (or the 8α-methyl group in FMN-containing samples) attached to C8 but also the two magnetically inequivalent protons attached to C1′ and the one attached to C6, four (or six in the case of FMN-containing samples) hfc's were fitted for 8-demethyl-FMN exchanged samples. The signs of hfc's cannot

(27) Ortiz-Maldonado, M.; Ballou, D.; Massey, V. *Biochemistry* **1999**, *38*, 8124–8137.
(28) Stoll, S.; Schweiger, A. *J. Magn. Reson.* **2006**, *178*, 42–55.

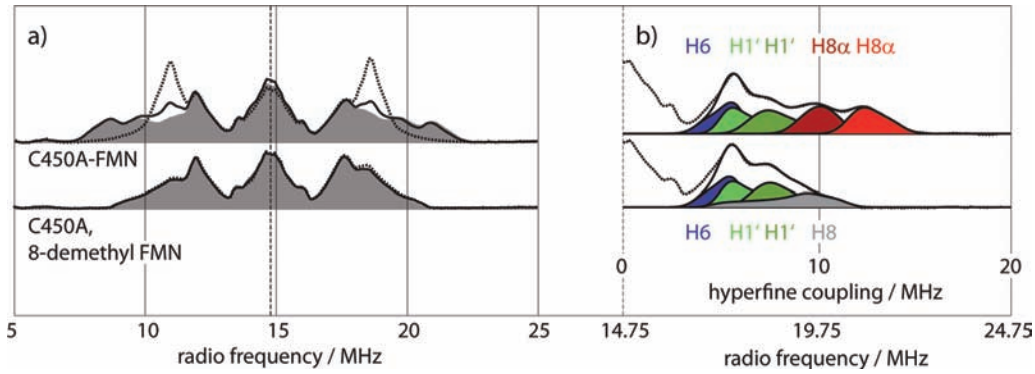


***Figure 2.*** (a): Pulsed X-band proton Davies ENDOR spectra taken at the peak intensity of the respective field-swept echo spectra and corrected with respect to the proton Larmor frequency at each field position. Spectra were recorded at three different temperatures each (120 K, dashed line; 80 K, black line; 10 K, gray shaded) for *As*LOV2 C450A and 8-demethyl-FMN *As*LOV2 C450A neutral radicals. (b) Details of the *As*LOV2 10 K spectra from 0 MHz to about 20 MHz hfc's with accompanying spectral simulation of the outer part of the spectrum (measured spectrum, dashed line; single simulated hfc's, shades of blue, green, and red; envelope of simulated hfc's, black line). For details, see text.

***Table 1.*** Isotropic Proton Hyperfine Couplings of the FMNH• Cofactors Obtained from Simulations of the Symmetrized Pulsed ENDOR Spectra of Mutant *As*LOV2 Domains Measured at 10 K[a]

| *As*LOV2 C450A | | *As*LOV2 C450A/L496V | | *As*LOV2 C450A/F509V | | *As*LOV2 C450A/N425S | | *As*LOV2 C450A 8-demethyl-FMN | | *As*LOV2 C450A/L496A | | *As*LOV2 C450A/F509A | | *As*LOV2 C450A/N425C | |
|---|---|---|---|---|---|---|---|---|---|---|---|---|---|---|---|
| | $A_{iso}$ | | $A_{iso}$ | | $A_{iso}$ | | $A_{iso}$ | | $A_{iso}$ | | $A_{iso}$ | | $A_{iso}$ | | $A_{iso}$ |
| H6 | −5.3 | H6 | −5.3 | H6 | −5.1 | H6 | −5.3 | H6 | −5.2 | H6 | −5.4 | H6 | −5.2 | H6 | −5.3 |
| H1′ | 6.3 | H1′ | 6.4 | H1′ | 6.2 | H1′ | 6.3 | H1′ | 6.2 | H1′ | 6.3 | H1′ | 6.2 | H1′ | 6.1 |
| H1′ | 7.8 | H1′ | 7.9 | H1′ | 7.5 | H1′ | 7.4 | H1′ | 7.8 | H1′ | 8.9 | H1′ | 7.7 | H1′ | 8.3 |
| H8α | 10.2 | H8α | 10.1 | H8α | 9.3 | H8α | 9.0 | H8 | 8.6 | H8α | 10.2 | H8α | 9.5 | H8α | 6.3 |
| H8α | 12.8 | H8α | 12.7 | H8α | 13.5 | H8α | 12.6 | | | H8α | 12.0 | H8α | 13.2 | H8α | 14.9 |
| | | | | | | | | | | | | H8α (iso) | 7.8 | H8α (iso) | 7.9 |

[a] All values in MHz; signs of hyperfine couplings have not been determined experimentally but were taken from theoretical calculations.[29,30] The experimental errors are ±0.05 MHz for all components. Two protein samples, *As*LOV2 C450A/F509A and *As*LOV2 C450A/F509A, require another hyperfine component for exact spectral fitting. This tensor represents hyperfine couplings from a rotating 8α-methyl group and is denoted as H8α(iso).

be determined directly by ENDOR spectroscopy; therefore, they were taken from theoretical calculations.[29,30]

An axial hf tensor for H6 with principal values $A_{||}(H6) = -3.8$ MHz and $A_{\perp}(H6) = -5.9$ MHz (thus yielding an isotropic hfc constant of $A_{iso}(H6) = (A_{||}(H6) + 2A_{\perp}(H6))/3 = -5.2$ MHz), two slightly rhombic tensors for both 1′-protons (with an isotropic hfc of $A_{iso}(H1') = (A_1(H1') + A_2(H1') + A_3(H1'))/3 = 6.2$ and 7.8 MHz, respectively), and a strongly anisotropic hf tensor for the proton located at C8 (with an isotropic hfc constant of $A_{iso}(H8) = 8.6$ MHz) are the fitting result for the experimental ENDOR data of 8-demethyl *As*LOV2 C450A (see also Table 1, Supporting Information Table 1, and Figure 2b). The shapes of the H6 and H1′ hf tensors are in line with recently published data from other flavosemiquinone radicals,[16,31−34] thus confirming the quality of the spectral simulations. Moreover, ENDOR data on the H8 proton in 8-demethyl FMN have not yet been reported. Generally, a strongly anisotropic hf tensor is expected for α-protons, which is consistent with our experimental data (see Supporting Information Table 1 and Figure 2b).

For FMN-containing *As*LOV2 C450A samples we expected no significant change of the hfc's arising from H1′ and H6, as the 8α-methyl group is rather distant from H6, and changes at this side of the isoalloxazine moiety should not significantly alter hfc's of more remote protons. Therefore, we performed simulations with the parameters obtained from spectral simulation of 8-demethyl-FMN *As*LOV2 (see also Table 1 and Figure 2a). Both H1′ and H6 hfc's ($A_{iso}(H6) = -5.3$ MHz; $A_{iso}(H1') = 6.3$ and 7.8 MHz, respectively) are, within experimental error, identical to the ones obtained from 8-demethyl-FMN. In contrast to spectral fittings of ENDOR data obtained from 8-demethyl-FMN-substituted *As*LOV2 C450A samples, two additional hfc's with isotropic parts ($A_{iso(1)}(H8\alpha) = 10.2$ MHz and $A_{iso(2)}(H8\alpha) = 12.8$ MHz) could now be detected in the 10 K spectrum of FMN-containing *As*LOV2 C450A samples. These can be assigned to two, at such low temperature arrested, and thus magnetically inequivalent 8α protons. As the hf tensor $A_{meth}$ of a freely rotating methyl group is the average of the three individual proton hf tensors $A_i$, with $i = 1$, 2, or 3, $A_{meth} = (A_1 + A_2 + A_3)/3$, and an isotropic part $A_{iso,meth} = (A_{iso,1} + A_{iso,2} + A_{iso,3})/3$, it is perspicuous that the third proton assumes a very small hyperfine constant, $A_{iso,3} = 3A_{iso,meth} - (A_{iso,1} + A_{iso,2}) \approx 0$ MHz. Therefore, the resonances of this specific proton cannot be easily assigned from our ENDOR data, as many weakly coupled protons are overlapping in this region. Consequently, only two of the three 8α-protons will be used for further discussions.

(29) García, J. I.; Medina, M.; Sancho, J.; Alonso, P. J.; Gómez-Moreno, C.; Mayoral, J. A.; Martínez, J. I. *J. Phys. Chem. A* **2002**, *106*, 4729–4735.
(30) Weber, S.; Möbius, K.; Richter, G.; Kay, C. W. M. *J. Am. Chem. Soc.* **2001**, *123*, 3790–3798.
(31) Barquera, B.; Ramirez-Silva, L.; Morgan, J. E.; Nilges, M. J. *J. Biol. Chem.* **2006**, *281*, 36482–36491.
(32) Okafuji, A.; Schnegg, A.; Schleicher, E.; Möbius, K.; Weber, S. *J. Phys. Chem. B* **2008**, *112*, 3568–3574.
(33) Kay, C. W. M.; Feicht, R.; Schulz, K.; Sadewater, P.; Sancar, A.; Bacher, A.; Möbius, K.; Richter, G.; Weber, S. *Biochemistry* **1999**, *38*, 16740–16748.
(34) Çinkaya, I.; Buckel, W.; Medina, M.; Gómez-Moreno, C.; Cammack, R. *Biol. Chem.* **1997**, *378*, 843–849.

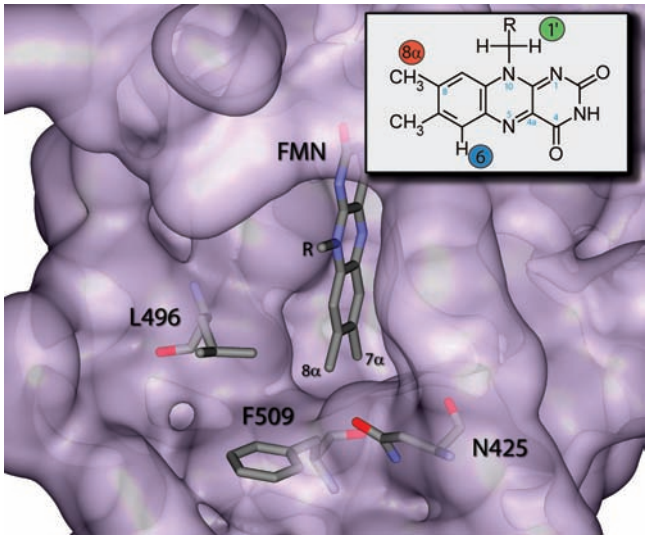


***Figure 3.*** FMN binding site of *As*LOV2 C450A. Coordinates were taken from 1G28. Inset: Structure based on the IUPAC nomenclature of the riboflavin molecule. The positions of the protons H1′, H6, and H8α are indicated with green, blue, and red, respectively.

**Design of Binding-Pocket Mutants.** According to crystallographic data,[35] we have identified three amino acids localized nearby the 8α-methyl group of FMN (see Figure 3). Point mutations of all three amino acids were introduced, and the recombinant proteins were investigated with proton pulsed-ENDOR spectroscopy.

The mutations were designed to alter steric restrictions in the vicinity of the 8α-methyl group of FMN. In a second approach, all three amino acids were mutated to the respective amino acid present in LOV1 domains from *C. reinhardtii*. Phe509 is conserved in nearly all LOV domains and was mutated to valine and alanine, respectively. Due to the exchange of the phenyl moiety with less bulky residues in the case of valine, and in particular in the case of alanine, the environment of the 8α-methyl group is expected to become less space-filling. Therefore, differences in the temperature dependence are expected. The second amino acid, Leu496, is also highly conserved among all LOV2 domains. On the other hand, most LOV1 domains have a valine at this position. Therefore, two mutations were constructed, one changing leucine to valine (simulating a LOV2-to-LOV1 exchange) and the other changing the bulkier leucine to the smaller alanine. The third amino acid, Asn425, which is only partly conserved in LOV2 domains, was mutated to cysteine, a residue that is found both in LOV1 and LOV2 domains from *C. reinhardtii*. Moreover, asparagine was replaced with the less bulky serine. The motivation for this mutation is that there is no change in the oxygen side-group atom, which points, according to crystal structures, toward the 8α-methyl group.[35,36]

The cognate recombinant proteins were expressed in an *E. coli* host strain and purified by nickel chelating chromatography. Their absorption spectra were closely similar. Aside from minimal changes in the extinction coefficient of the band at 447 nm, neither shifts nor additional bands could be detected (data not shown). All proteins were investigated with pulsed proton-ENDOR spectroscopy.

(35) Halavaty, A. S.; Moffat, K. *Biochemistry* **2007**, *46*, 14001–14009.
(36) Crosson, S.; Moffat, K. *Proc. Natl. Acad. Sci. U.S.A.* **2001**, *98*, 2995–3000.

Compared to spectra from *As*LOV2 C450A samples, substantial changes in the general appearance and in their temperature dependence are expected. Therefore, all double-mutant *As*LOV2 samples were characterized in terms of their temperature behavior and their, at 10 K, simulated hfc's in more detail, and compared with values obtained from *As*LOV2 C450A and *Cr*LOV2 samples. All ENDOR spectra recorded at 120, 80, and 10 K, including their spectral simulations, are summarized in Figure 4 (their isotropic hfc's are listed in Table 1, and the anisotropic hf components are listed in Supporting Information Table 1). Moreover, a different visualization of their temperature characteristics is plotted in Figure 5: the ratios between rotating and arrested 8α-methyl-group hfc's were calculated from spectral simulations for all three temperatures, normalized and plotted against the sample number, thus enabling a direct comparison between all samples.

In detail, L496V, which is the most conservative mutation, results in almost identical ENDOR spectra from which isotropic hfc's ($A_{iso}$(H6) = −5.3 MHz, $A_{iso}$(H1′) = 6.3 and 7.8 MHz, $A_{iso(1)}$(H8α) = 10.1 MHz, and $A_{iso(2)}$(H8α) = 12.7 MHz) have been extracted by spectral simulation that are nearly identical to those of the *As*LOV2 C450A protein. Moreover, comparison of C450A and C450A/L496V spectra recorded at the three different temperatures exhibits an almost identical temperature behavior (Figure 5). In contrast, spectra of C450A/L496A recorded at 10 K show a decrease by more than 1 MHz of the outer shoulder of the hyperfine structure. Spectral fittings show significant changes in the strength of the two H8α hfc's ($A_{iso}$(H8α) = 9.3 MHz and $A_{iso}$(H8α) = 13.5 MHz). Conversely, the temperature dependence of this mutant sample remains essentially comparable to that of the C450A sample: at 120 K, the methyl rotation is fast on the ENDOR time scale, thus producing just one averaged hfc tensor, while at 80 K two of three hf tensors of the H8α protons become distinguishable. Spectra recorded at 10 K provide two fully resolved proton hfc's as the three formerly averaged H8α tensors are now arrested and therefore become magnetically inequivalent.

Mutation of the F509 position, on the other hand, results in drastic changes for both constructs. In spectra recorded at 80 K, both C450A/F509V and C450A/F509A samples show a very broad—hence shallow—peak of one H8α proton with an hfc of 13.5 MHz, while retaining a strong fraction of the averaged 8α-tensor. At 10 K, the C450A/F509V spectrum can be simulated with locked-in methyl-group protons, whereas in the C450A/F509A spectrum, a significant number of methyl-group protons still remain rotating freely (orange hyperfine component in Figure 4b). This result is not unexpected as alanine is less space-filling as compared to valine, thus reducing potential methyl-group restrictions by the protein. This is consistent with the different temperature behavior. At 10 K, both isotropic 8α hfc's are nearly identical: $A_{iso(1)}$(H8α) = 9.3 MHz and $A_{iso(2)}$(H8α) = 13.5 MHz for C450A/F509V, and $A_{iso(1)}$(H8α) = 9.5 MHz and $A_{iso(2)}$(H8α) = 13.2 MHz for C450A/F509A. Nevertheless, the peak at 13.5 MHz appears much broader in the C450A/F509A sample. One possible explanation for this unusual spectral pattern could be that there is no clear preference of one dihedral angle in this specific mutation. Therefore, a broad distribution of different angles (the dihedral angle of the C−H bond with respect to the ring plane axis) overlaps, which results in this observed spectral pattern. In general, spectral line

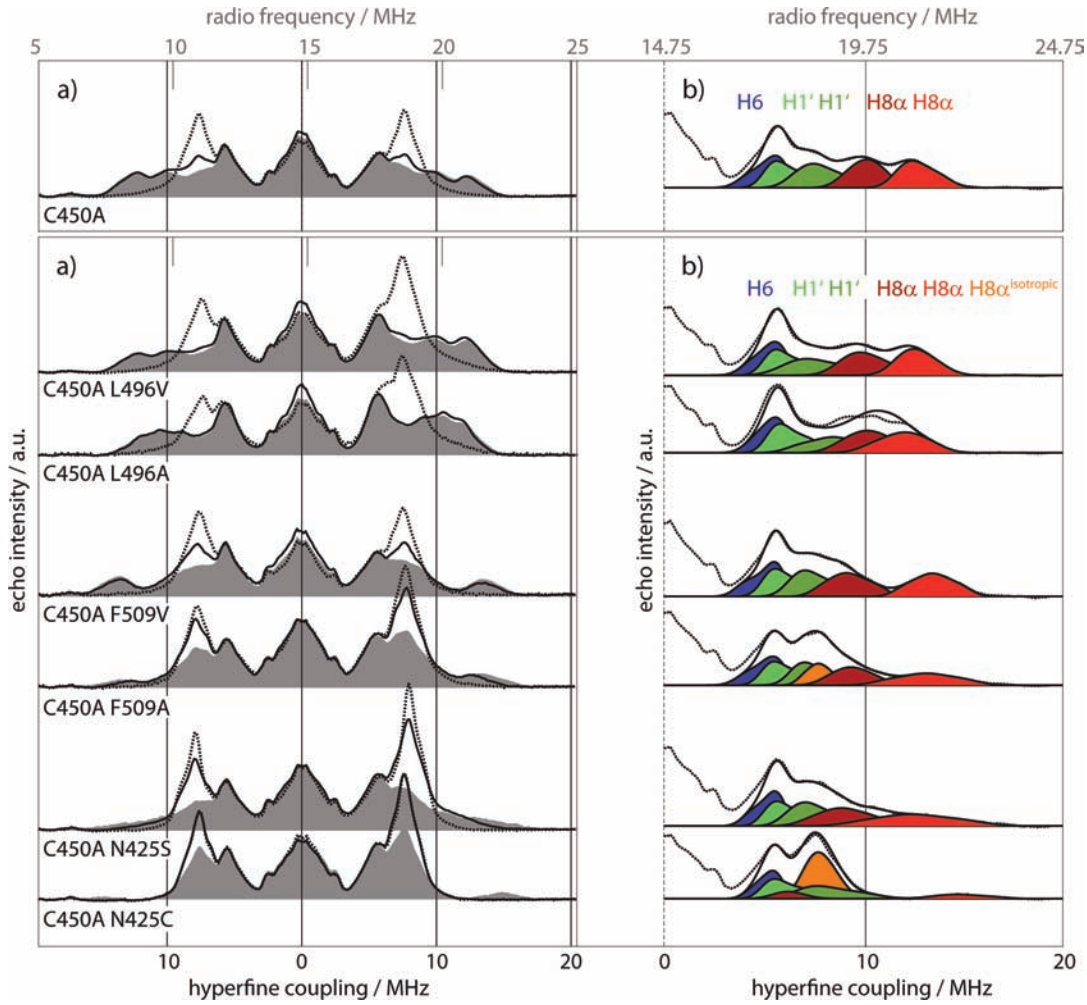


***Figure 4.*** (a) Pulsed X-band proton Davies ENDOR spectra of various *As*LOV2 double-mutants taken at the peak intensity of the respective field-swept echo spectra. Spectra were recorded at 120 (dashed line), 80 (black line), and 10 K (gray line) for *As*LOV2 C450A double-mutants described in the text. (b) Extract of the *As*LOV2 10 K spectra from 0 to about 20 MHz hfc's with accompanying spectral simulation of the outer wing of the spectrum (measured spectrum, dashed line; single simulated hfc's, shades of blue, green, and red; envelope of simulated hfc's, black line). Two protein samples, *As*LOV2 C450A/F509A and *As*LOV2 C450A/N425C, require another hyperfine component of axial symmetry for exact spectral fitting. This feature, shown in orange, represents hfc's from fast-rotating 8α-methyl-group protons and is denoted as H8α(iso). For further details, see text.

broadening of hfc's due to overlapping of microconformations is named "*A*-strain".[37]

Samples containing mutations at the N425 positions exhibit other significant changes. First, both the temperature characteristics and the spectrum at 10 K of the C450A/N425S sample ($A_{iso(1)}$(H8α) = 9.0 MHz and $A_{iso(2)}$(H8α) = 12.6 MHz) are more similar to those obtained from the samples with a mutation at position F509 than at position L496. However, the hfc (arising from one of the 8α-protons) centered at 12.5 MHz exhibits a very strong *A*-strain, thus suggesting that the conformational freedom is much larger than, e.g., in the C450A/F509A sample. C450A/N425C, on the other hand, shows a similar temperature behavior that is comparable only to that of the C450A/F509A sample. At 120 and 80 K, most of the 8α-methyl groups remain mobile; no additional shoulder around 12 MHz can be detected. Even at 10 K, a small additional peak arises outside the main ENDOR signal of the H8α group but has only ∼35% integral intensity compared to the intensity of other samples (see Figure 5). In addition, it has to be mentioned that the peak centered at 14.9 MHz exhibits the strongest hfc of all investigated samples (see also Table 1). Moreover, a clearly reduced *A*-strain (as compared to the C450A/F509A and C450A/N425S samples), suggesting a defined position of the 8α-protons, is observed, which is confirmed by spectral simulations. Inspection of Figures 4 and 5 leads to a second, unexpected result: by comparing the ENDOR spectra and the temperature profile of the C450A/N425C sample with those of all other samples, clear similarities between the two parameters can only be detected with *C. reinhardtii* LOV2 C250S. For the latter, all ENDOR spectra show surprisingly similar behavior not only at 10 K but also at 80 and 120 K.

**Estimating Dihedral Angles via Density Functional Theory Calculations.** With precise hfc parameters from two of the three 8α-protons at hand, the angles of the respective C−H bonds with respect to the isoalloxazine's ring plane can now be determined using DFT calculations. For this purpose, we calculated the ENDOR parameters of the neutral flavin radical as a function of the dihedral angle of the 8α-methyl group (calculations were performed in 10° steps of 8α-rotation). The results for the three isotropic hfc values depending on the rotation angle with respect to their original orientation are shown in Figure 6 (the 0° position has been chosen arbitrarily as the

(37) Hagen, W. R. *Biomolecular EPR Spectroscopy*; CRC Press, Taylor & Francis Group: Boca Raton, FL, 2008.

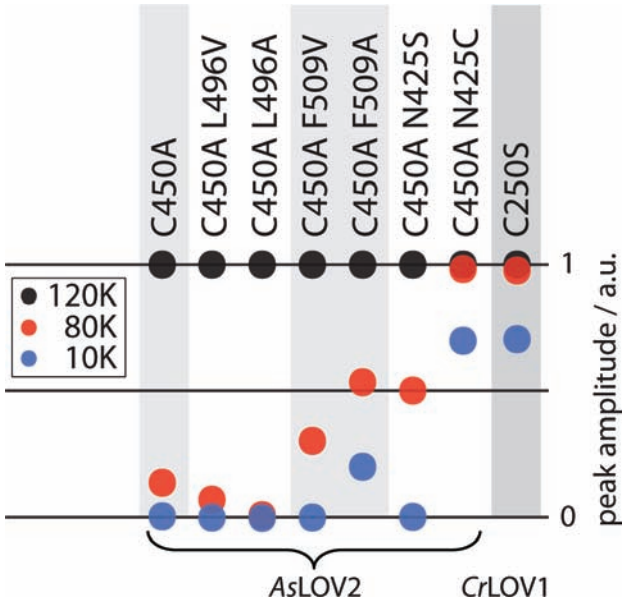


***Figure 5.*** Ratios between rotating and arrested 8α-methyl-group hfc's, extracted from spectral simulations for all three temperatures, normalized and plotted against the sample number, thus enabling a direct comparison of all samples. Values have been extracted from Figures 1, 3, and 4. Data extracted from 120 K spectra are shown in black, red for 80 K spectra, and blue for 10 K spectra.

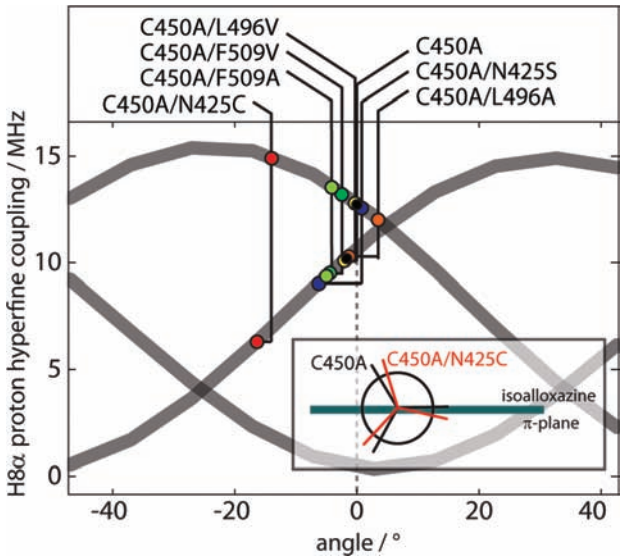


***Figure 6.*** Hyperfine coupling values of the three H8α protons as a function of the rotation angle from DFT calculations (for details, see the text). In gray, the isotropic part of the calculated hyperfine tensor for each of the three hydrogens is shown. Different colored dots mark the isotropic hyperfine values for two 8α protons obtained by spectral simulation of the experimental data. Inset: Graphical view showing the angles of the three 8α-methyl-group protons with respect to the isoalloxazine ring plane. For clarity, only two selected samples, *As*LOV2 C450A and *As*LOV2 C450A/N425C, are shown.

position of the 8α-methyl group that was returned from an energy optimization of the structure).

The calculation shows a quasi-sinusoidal behavior (as expected according to the empirical Heller−McConnell relation[38]). The deviation of the isotropic hyperfine values (shown in gray lines) from a sinusoidal function of roughly 0.5 MHz is expected

(38) Heller, C.; McConnell, H. M. *J. Chem. Phys.* **1960**, *32*, 1535–1539.

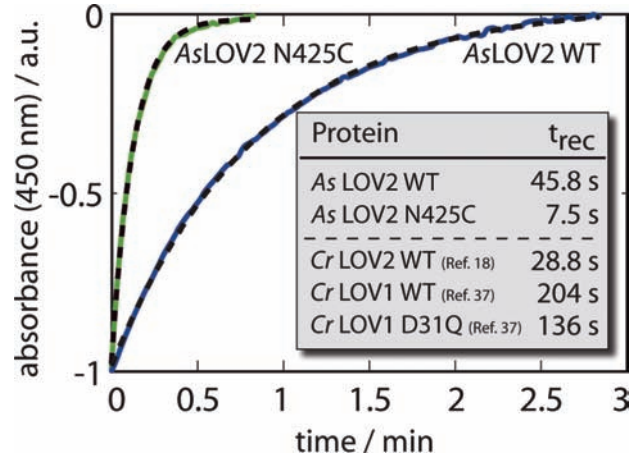


***Figure 7.*** Light-state lifetime of *As*LOV2 WT (blue line) and AsLOV2 N425C (green line) mutants. Spectral fittings with a monoexponential decay curve are shown as dashed lines. Inset: Experimental data are compared with dark recoveries from selected LOV domains obtained from the literature.[19,42]

to be caused by the asymmetric protein surrounding. The dihedral angle of the H8α group locked at low temperatures in the mutants can be read out from the plot by searching the angle fitting best with the two experimentally determined isotropic hfc values (see Table 1). It has to be mentioned, however, that this procedure is only applicable within a range of 30°, as the three individual methyl-group protons are equivalent.

Angular differences are observed, which we have compiled in the Supporting Information Table 2. A dihedral angle of (+1 ± 2)° is observed for *As*LOV2 C450A; additional mutation of the amino acid Leu496 leads to only subtle changes of this angle ((+3 ± 5)° for C450A/L496V and (−1 ± 2)° for C450A/L496VA). Similarly, mutations of Phe509 (either to valine or to alanine) afford only a small decrease of this angle (C450A/F509V, (−2 ± 2)°; C450A/F509A, (−3 ± 1)°). The situation is different for the replacement of Asn425, where the N425S mutation also leads to a minor change (−1 ± 7)°; however, the error bar in the N425S mutant is larger than for the other six mutants. Furthermore, the angle is significantly downshifted to −13 ± 2° in the N425C sample. This angular change can only be rationalized if the local environment is altered considerably. The exchange of the asparagine residue with a cysteine seems to change not only the steric environment but also the strength of polar interactions and/or hydrogen bonds. These results will be discussed in more detail below.

**UV−Vis Dark-Recovery Assay.** To test the influence of the Asn425 residue for photochemical activity, an *As*LOV2 sample comprising an Asn425-to-Cys replacement was generated, overexpressed, and purified under similar conditions. As this sample is capable of FMN-4a-adduct formation, we recorded the photoreceptor's dark recovery with optical spectroscopy and compared it with data obtained from *As*LOV2 wild-type (WT) samples measured under identical experimental conditions. Monoexponential fitting of the back-reaction of the N425C mutant results in an adduct-state lifetime $\tau_{rec(N425C)}$ of 7.5 s, which is 7-fold decreased as compared to that of the WT ($\tau_{rec(WT)}$ = 45.8 s). These results are, together with published adduct-state lifetimes from comparable LOV domains (and LOV1−LOV2 constructs), depicted in Figure 7.

## Discussion

Proton-ENDOR spectroscopy provides information on the electronic structure of hydrogens through the detection of hfc's

arising from the interaction of magnetic nuclei with the unpaired electron spin. As hfc's are strongly modulated by interactions with the close environment, hydrogen bonds and their strength can be evaluated with this method. Although information on the delocalization of the unpaired electron spin in the aromatic isoalloxazine ring of flavins is not directly obtained from proton hfc's, they may nevertheless be used to map the spin density located on carbon and nitrogen nuclei of the conjugated $\pi$-system of the isoalloxazine ring by using McConnell's equation, $a_k = C\rho_k$[38] (where $a_k$ is the (isotropic) hfc constant of a proton attached to an atom $k$ which has a spin population $\rho_k$ in an orbital that contributes to the isoalloxazine's $\pi$-system; $C$ is a proportionality constant). All six investigated double-mutant proteins show similar $A_{iso}$ values of all assigned proton positions (see Table 1), thus reflecting similar electron-spin density distributions of the FMN cofactor.

In general, an assignment of the individual hfc components arising from protons that interact with the unpaired electron spin is rather difficult because of the high anisotropy of the hyperfine tensor $A$ in randomly oriented, diffusion-limited samples. Therefore, spectral components of the proton hfc's overlap to a certain extent. Increasing the magnetic field (and thereby increasing the electron Zeeman interaction) is often used for assigning hfc's with the help of the so-called "orientation selection" effects. Exciting only defined molecules in a non-oriented frozen-solution sample reduces the number of resonances in the sample and, therefore, increases the uniqueness of the assignment. Unfortunately, the **g**-anisotropy of the flavin molecule is very low.[39] Consequently, orientation selection is not very efficient, as the **g**-tensor remains only partially resolved, even at W-band frequencies. A different approach is to reduce the number of resonating protons by chemically altering the flavin molecule. Here, we investigate an 8-demethyl-FMN-exchanged *As*LOV2 sample as an artificial model compound for the assignment of proton hfc's. In combination with DFT calculations of hfc's, the use of this model compound allows an unambiguous spectral simulation of the protons H1′ and H6. Assuming only minor changes of the hfc's, the proton-ENDOR spectrum arising from *As*LOV2 C450A protein with FMN cofactor is no longer under-determined, and the proton hfc's arising from the three, locked-in and thus magnetically inequivalent 8α protons can be extracted.

With these hfc values at hand, we investigated the temperature dependence of different LOV domains. Whereas *Cr*LOV2 samples show a temperature behavior common to other flavoproteins (a slowly decreasing integral of the axial hyperfine tensor from the three methyl-group protons upon cooling), *As*LOV2 samples lead to a significantly decreased rotational motion of the 8α-methyl protons with respect to the ENDOR time scale (which is in the microsecond range), even at elevated temperatures.

Figure 5 shows qualitatively the different temperature behavior of *As*LOV2 samples (including most of the investigated mutant samples) compared to the *Cr*LOV2 sample with respect to the methyl-group dynamics. In *Cr*LOV2 C250S and *As*LOV2 C450A/N425C samples, the contribution of the freely rotating 8α-methyl group remains unaltered between 120 and 80 K, and even at 10 K about 65% of the methyl groups still show a motionally averaged hfc. In *As*LOV2 C450A/F509A the fraction of mobile 8α-methyl groups drops to about 50% between 120 and 80 K and decreases further to about 20% at 10 K. Determining whether this remaining fraction of motionally averaged 8α-methyl groups represents a thermally activated rotation or a tunneling process is not possible on the basis of our present data but clearly deserves further investigation.

The other *As*LOV2 mutant samples show a variable degree of mobile 8α-methyl groups at 80 K. This indicates different activation energies for the methyl-group rotation in these samples. Almost no contribution of mobile 8α-methyl groups is detected in the two *As*LOV2 C450A/L496 mutants (A and V) already at 80 K. This situation is reached in the other mutants at 10 K. Thus, we can conclude that, in all samples except *Cr*LOV2, *As*LOV2 C450A/N425C, and *As*LOV2 C450A/F509A, any 8α-methyl-group dynamics, including tunneling, is slower than probed by X-band ENDOR.

Sequence and structural alignments of various LOV domains show that the flavin binding pocket is highly conserved among the two LOV proteins under investigation.[12,40] Therefore, rather small topological changes have to be responsible for this unexpected temperature effect. With the hfc values from the H1′ and H6 protons, spectral simulation of the two distinguishable 8α protons can be achieved. Point mutations in the direct vicinity of these protons led to various spectral changes. Results obtained from spectral simulations of the individual hfc's of LOV samples shown in Figure 4 can be divided in two parts. (i) Point mutations of specific amino acid residues change the temperature dependence of the arrested methyl group in *As*LOV2. Proteins containing mutations in amino acid Leu496 do not seem to have strong interactions with the 8α-protons, as the spectra recorded at 120, 80, and 10 K are highly comparable to those of *As*LOV2 C450A samples. On the other hand, mutations of Phe509 and in particular Asn425 lead to a drastically altered temperature behavior, which is illustrated in Figure 4a and in Figure 5. Conservative mutations such as F509V cause only subtle changes, whereas F509A, N425S, and especially N425C show an increase in rotational freedom of the methyl group even at 10 K, which makes spectra of the latter mutation highly comparable to those obtained from *Cr*LOV2 samples (see Figure 1b and Figure 4a). (ii) Point mutations of specific amino acid residues change the angle of the arrested 8α-methyl protons with respect to the isoalloxazine ring plane. Assisted by DFT calculations, these dihedral angles could be precisely determined (see Supporting Information Table 2). Compared to the C450A samples, mutations of Leu496 lead to a minor decrease of this angle, whereas mutations of Phe509 increase this angle slightly. On the other hand, mutations of Asn425 change the angle dramatically: whereas the angle in N425S samples is only moderately increased, N425C mutations changed the dihedral angle by about 10° (the angle difference between *As*LOV2 C450A and *As*LOV2 C450A/N425C samples is further illustrated in the inset of Figure 6).

A more detailed picture of how the three amino acids interact with the 8α-methyl group can be drawn by combining the above-mentioned results. Sequence alignments show that virtually all LOV domains harbor a hydrophilic amino acid at position 496. Nevertheless, their interaction with the isoalloxazine moiety seems marginal, as both mutant samples do not show any substantial changes compared to the *As*LOV2 C450A protein alone. On the other hand, Phe509 is highly conserved in all LOV domains and has a significant influence on the 8α-methyl-group interaction. Exchanging Phe509 with less bulky

(39) Fuchs, M.; Schleicher, E.; Schnegg, A.; Kay, C. W. M.; Törring, J. T.; Bittl, R.; Bacher, A.; Richter, G.; Möbius, K.; Weber, S. *J. Phys. Chem. B* **2002**, *106*, 8885–8890.

(40) Crosson, S.; Rajagopal, S.; Moffat, K. *Biochemistry* **2003**, *42*, 2–10.

residues is conducive to a remarkable alteration of their temperature dependence and in an increase of *A*-strain. This can be rationalized by taking enhanced conformational flexibility of the FMN cofactor into account. The third amino acid (Asn425) surrounding the 8α-methyl group is conserved in LOV2 but not in LOV1 domains. Exchanging this amino acid residue with either cysteine or serine results in two different changes in the ENDOR spectra: First, *As*LOV2 C450A/N425S samples show the strongest *A*-strain in the ENDOR spectra, thus having the highest conformational flexibility of all investigated samples (see Figure 4). Second, *As*LOV2 C450A/N425C samples show only minute *A*-strain (see Figure 4) but a dramatically altered dihedral angle, as depicted in Figure 6. These findings support the idea that each 8α-methyl group in the two samples assumes a different conformation. Asn425Cys samples seem to restrict the conformational freedom of the isoalloxazine moiety—hence in a different conformation than in the *As*LOV2 C450A protein—while Asn425Ser samples seem to increase conformational flexibility. One reasonable explanation for these finding is that Ser425 and Cys425 assume different conformations with respect to the isoalloxazine moiety.

Accordingly, we were able to identify Asn425 as an important amino acid for the interaction with the xylene ring of the flavin cofactor. To test the influence of this amino acid for photochemical activity, *As*LOV2 N425C samples were investigated with optical spectroscopy. The light-state lifetime of *As*LOV2 was determined to be $\tau_{rec(WT)} = 45.8$ s, which is clearly similar to published data.[12] *As*LOV2 N425C samples, on the other hand, showed significantly altered chemical stability of the light-state reactivity; its light-state lifetime is decreased by a factor of 7 ($\tau_{rec(N425C)} = 7.5$ s) when measured under identical experimental conditions (see Figure 7). Published data from various LOV domains from different organisms imply that the dark-recovery of LOV2 domains is in general much faster than that of LOV1 domains, in the range of 30−60 s.[12,19,41,42] Although some mutated LOV domains with altered photochemical behavior have been published, a 7-fold decrease of the cysteinyl-4a adduct lifetime from mutations in the direct surrounding of the FMN cofactor has not yet been achieved. Therefore, it is obvious from our experiments that this particular amino acid has a significant influence on the stability of the light state in LOV domains, even if the amino acid is not located in the direct vicinity of the photoreceptor's reactive site. Although there is no direct correlation between the observed temperature dependence of methyl-group rotation and the cysteinyl-4a adduct stability, we are able to propose a hypothesis for these observed changes in *As*LOV2 N425C samples. Interaction between Asn425 and the 8α-methyl group seems to "coerce" the isoalloxazine moiety into one specific conformation, thus stabilizing the intrinsically weak C−S bond of the cysteinyl-4a adduct. On the other hand, mutating this amino acid leads to an increase of conformational flexibility of the flavin cofactor and, thus, to a destabilization of the S−C(4a) bond, and ultimately to the observed dramatic decrease in dark-state recovery rate.

## Conclusions

In this contribution we describe how low-temperature ENDOR studies of blue-light-active phototropins can be used to gain information on the FMN cofactor's direct vicinity and to estimate the strength of protein−cofactor interaction. In detail, (i) we were able to detect a unique spectral behavior of *As*LOV2 C450A samples as their 8α-methyl-group motion is restricted starting at elevated temperatures ($T > 110$ K); (ii) with a mutagenesis study in the close vicinity of the 8α-methyl group, we were able to identify amino acids responsible for enhanced (and reduced) protein−cofactor interaction, resulting in altered sterical interaction; (iii) mutations in these amino acids showed clearly changed temperature behavior, which is in line with the observed altered sterical interaction; (iv) spectral assignment in combination with DFT calculations resulted in a precise determination of the orientation of the methyl group with respect to the isoalloxazine ring plane; and (v) as an additional output of this ENDOR study, Asn425 could be identified as an important amino acid for photochemistry of LOV domains.

In general, there is a growing importance to unravel subangstrom interactions in order to understand enzyme-mechanistic details. Temperature-dependent ENDOR spectroscopy can assist in unscrambling these subtle protein−cofactor interactions.

## Experimental Section

**Protein Preparation.** LOV domains from *A. sativa* and *C. reinhardtii* were expressed and purified using published procedures.[24,43,44]

**Preparations of LOV Domain Point Mutations.** Site-directed mutagenesis of double-mutant *As*LOV2 domains were performed as described earlier.[45] Plasmid pNCO-HAC-CYS-ASL2EC-REP-6, which carries a C450A mutation, was used as a template. For generation of the *As*LOV2 N425C clone, plasmid pNCOHAC-L2-AS-WT was used as template. Primers used for mutagenesis are shown in Table 2.

**Preparation of 8-Demethyl-FMN.** 8-Demethylflavin was synthesized using a published procedure.[27]

**Generation of FMN Radicals in LOV Domains.** Samples containing 10 mM HEPES pH 7.0, 10 mM NaCl, 30% glycerol (v/v), 5 mM EDTA, and 0.5−0.7 mM protein were transferred into EPR quartz tubes (3 mm inner diameter) under an argon atmosphere in the dark. Subsequently, they were illuminated with blue light selected with a 420−470 nm band filter from a white light source at 277 K to generate the semireduced state of the FMN cofactor. Photoreduction progress was monitored using a Varian Cary 100 spectrophotometer. Samples were frozen rapidly and stored in liquid nitrogen.

**Dark-Recovery Kinetics.** All proteins were concentrated to ~70 μM in buffer containing 10 mM HEPES pH 7.0, 10 mM NaCl, and 10% glycerol (v/v). UV−visible absorbance spectra were measured on a Varian Cary 100 spectrophotometer at 450 nm. Kinetic experiments monitored the return of the 450 nm signal following blue-light illumination. Data points were fitted using a first-order rate equation to yield the light-state lifetime ($\tau_{rec}$).

**ENDOR Spectroscopy.** X-band pulsed ENDOR spectra were recorded using a commercial pulse EPR spectrometer Bruker E580 (Bruker BioSpin GmbH, Rheinstetten, Germany) in conjunction with a dielectric-ring ENDOR resonator Bruker ER 4118X-MD5-EN. For Davies-type ENDOR,[46] a microwave pulse sequence $\pi-t-\pi/2-\tau-\pi$ using 64 and 128 ns $\pi/2$ and $\pi$ pulses, respectively, and a radio frequency pulse of 10 μs duration starting 1 μs after the first microwave pulse were used. The separation times $t$ and $\tau$ between the microwave pulses were set to 13 μs and 500 ns, respectively. To avoid saturation effects due to long relaxation times,

(41) Guo, H.; Kottke, T.; Hegemann, P.; Dick, B. *Biophys. J.* **2005**, *89*, 402–412.
(42) Losi, A. *Photochem. Photobiol. Sci.* **2004**, *3*, 566–574.
(43) Holzer, W.; Penzkofer, A.; Fuhrmann, M.; Hegemann, P. *Photochem. Photobiol.* **2002**, *75*, 479–487.
(44) Holzer, W.; Penzkofer, A.; Susdorf, T.; Álvarez, M.; Islam, S. D. M.; Hegemann, P. *Chem. Phys.* **2004**, *302*, 105–118.
(45) Illarionov, B.; Kemter, K.; Eberhardt, S.; Richter, G.; Cushman, M.; Bacher, A. *J. Biol. Chem.* **2001**, *276*, 11524–11530.
(46) Davies, E. R. *Phys. Lett. A* **1974**, *47*, 1–2.

***Table 2.*** Oligonucleotide Primers Used for Site-Directed Mutagenesis of *LOV* Gene[a]

| no. | mutation | novel restriction site | nucleotide sequence (5′ → 3′) |
|---|---|---|---|
| 1 | none | none | CCA CGC GGA TCC GAA TTT |
| 2 | none | none | ATG TTC GGT ACC ATC CAA |
| 3 | N425C | *Msp*I | GAT AAT GGG **gca** ATC cGG CAA ACG TGG |
| 4 | N425S | *Msp*I | GAT AAT GGG **Aga** ATC cGG CAA ACG TGG |
| 5 | L496A | *Cvi*AII | GG AAC CTC TTT CAC **gcG** CAG CCc ATG CGT GAT CAG |
| 6 | L496V | *Cvi*AII | GG AAC CTC TTT CAC **gTt** CAG CCc ATG CGT GAT CAG |
| 7 | F509A | *Pvu*II | G TTC GGT ACC ATC CAg CTG GAC ACC AAT **cgc** GTA C |
| 8 | F509V | *Pvu*II | G TTC GGT ACC ATC CAg CTG GAC ACC AAT **AAc** GTA C |

[a] Primers 1, 3, 4, 7, and 8 were designed to hybridize to the sense DNA strand of *LOV* gene, and the rest of the primers to the antisense DNA strand. Mutated bases are indicated in lower case, and codons or anticodons specifying modified amino acid residues are shown in bold type. Novel restriction sites are underlined.

the entire pulse pattern was repeated with a frequency of only 142 Hz at temperatures down to 60 K. At even lower temperatures, the repetition rate had to be decreased further to 0.5 Hz because of the long relaxation times of the flavin chromophore. All ENDOR spectra were recorded at a magnetic-field value corresponding to the center-magnetic-field position of the X-band pulsed EPR signal shown in Supporting Information Figure S1.

**Data analysis.** All ENDOR spectra in this publication were normalized with respect to the radio frequency range from 11.7 to 12.8 MHz, the boundaries of the clearly pronounced peak of the H6 coupling which can be assumed to be thermally stable. Simulation of the spectra was carried out using the Matlab (The MathWorks, Natick, MA) package EasySpin (using "salt" simulation routine),[28] and the fitting was done with an in-house-written Matlab script.

**DFT Calculations.** Density functional theory calculations were carried out with Gaussian03 (Gaussian Inc., Pittsburgh, PA) by using the unconstrained compound functional B3LYP, the basis set EPR-II, and a tight model for the self-consistent field method. The input structure was based on the crystal structure LOV2.[36] It was then reduced to one layer of amino acids surrounding the flavin neutral radical. As cofactor, we used riboflavin instead of FMN. Moreover, the calculation effort could be significantly reduced by using EPR-II as basis set instead of EPR-III. The final input consisted of more than 100 atoms; hence, the option iop(6/82=1) had to be set.

Before the 8α group was manually rotated, the geometry of the whole setup was energetically optimized by letting the amino acids relax while holding their backbone positions fixed, and then relaxing the flavin cofactor again within its binding pocket.

**Acknowledgment.** We thank Dr. Chris Kay (University College of London) for assistance with the initial experiments and for helpful discussions. This work was supported by the Deutsche Forschungsgemeinschaft (Sfb-498, project B7).

**Supporting Information Available:** Complete proton hyperfine couplings of the $FMNH^{\bullet}$ cofactors obtained from spectral simulations and echo-detected EPR spectra of all LOV samples. This material is available free of charge via the Internet at http://pubs.acs.org.

JA910681Z